REMOTE SENSING OF ATMOSPHERIC FRONTAL DYNAMICS OVER THE OCEAN

Gad Levy[1] and Jerome Patoux[2]

[1]NorthWest Research Associates, Bellevue WA, [2]University of Washington, Seattle, WA USA gad@nwra.com

ABSTRACT. Frontal regions in midlatitude storms exhibit a wide range of behavior, which can be observed by remote sensors. These include decay, strengthening, rotating, and sometimes spawning of new cyclones. Here we refine and apply recent theories of front and frontal wave development to a case of a front clearly observed and analyzed in remote sensing data. By applying innovative analysis techniques to the data we assess the respective roles of ageostrophy, background deformation, and Boundary Layer processes in determining the evolution of the surface front. Our analysis comprises of diagnosis of the terms appearing in the vorticity and divergence equations using remotely sensed observations.

KEY WORDS: Marine Atmospheric fronts, Satellite winds, Boundary Layer dynamics

1. INTRODUCTION

Fronts have long been of interest to forecasters because they are often associated with significant weather changes, such as abrupt changes in pressure and temperature, precipitation, and shifts in the wind direction. They are characterized by higher vorticity, convergence, shear, and are inherently subject to instabilities.

Since Hoskins and Bretherton's (1972) seminal work on frontogenesis, numerous studies have delineated the role of deformation and shear in concentrating temperature gradients within frontal regions, as well as the role of ageostrophic circulations in accelerating frontogenesis (e.g., Hoskins, 1982; Keyser and Pecknick, 1985). Semigeostrophic (SG) theory captures the ageostrophic feedbacks restoring thermal wind balance in the frontal regions above the ABL. Within the ABL, however, turbulent fluxes of momentum and surface friction are of the same order of magnitude as the Coriolis acceleration, resulting in more complex frontal dynamics. Observations, primitive equation numerical solutions, and theoretical models suggest that the low-level flow around fronts is strongly modified by the ABL (Blumen, 1980; Thomson and Williams, 1997; Keyser and Anthes, 1982; Reeder and Smith, 1986; Levy, 1989).

Levy and Bretherton (1987) and Levy (1989) examined the surface dynamics of cold fronts by scaling and estimating different terms of the vorticity and divergence equations under different (idealized) conditions. They found that the ABL ageostrophy acts as a positive feedback mechanism that enhances vorticity and convergence growth. They also found that nonlinear terms can become important as the geostrophic deformation increases and can destabilize the frontal region. Levy (1989) found that the variation in stratification and thermal advection across the front favors the formation of stronger temperature gradients in cold fronts. The magnitude of the dynamic terms near the surface varies considerably across developmental stages of observed fronts, depending on the stratification, thermal advection, deformation and shear forcing. Levy hypothesized that frontogenesis is maximized at or slightly ahead of the cold front. Bannon and Salem (1995) examined the downward mixing of geostrophic momentum into the BL and the effect of thermal vorticity (i.e., vorticity of the thermal wind). They found that cyclonic thermal vorticity produces an increase in surface vorticity, whereas anticyclonic thermal vorticity produces convergence of the low-level warmward flow. Examining viscous effects, Xu and Gu (2002) find that surface drag is frontolytical in general, although the viscous part of the ageostrophic motion is indirectly frontogenetic and offset by the divergence of the dynamic part of the ageostrophic motion at the surface.

These findings, at times apparently contradictory, point to the complexity of frontal ABL dynamics and the interactions between ageostrophic circulation, surface drag, baroclinicity, and stratification in the ABL.

Developments in observational technology from space in recent decades have contributed significantly to identifying some of the complexities in frontal dynamics. For example, the resolution of the scatterometer winds (presently 25 km, with a 12.5-km experimental data set available) now allows us to detect mesoscale features and to study surface frontogenesis in greater detail (Zierden et al., 2000; Yeh et al., 2002). The current study takes advantage of the nature, resolution and coverage of the scatterometer data sets to better characterize the life cycle of an observed front near the surface in one North Pacific case study. It outlines a methodology that allows the use of the remote sensing technology to assess and improve recent theories of frontal development

2. FRONTAL PROCESSES

2.1 Vorticity and divergence equations

Consider the scaled vorticity and divergence equations near the surface (Levy and Bretherton, 1987):

$$\frac{dq}{dt} = -(f+q)D + F_q \qquad (1)$$

$$\frac{dD}{dt} = f(q - q_g) - (U_x^{\,2} + 2V_xU_y + V_y^{\,2}) + F_D \quad (2)$$

where q is the vertical component of the relative vorticity, D the divergence, q_g the geostrophic relative vorticity, U and V the horizontal components of the wind vector, the subscripts x and y represent the partial derivatives with respect to x and y and F_q, F_D represent the dissipation by surface drag.

The relationship of the vorticity and divergence in (1) and (2) to the evolution of the cross-front temperature gradient (frontogenesis) can be elucidated by considering the frontogenesis equation in terms of strengthening temperature gradient:

$$\frac{d}{dt}\left(\frac{\delta\theta}{\delta x}\right) = -D\left(\frac{\delta\theta}{\delta x}\right) - q\left(\frac{\delta\theta}{\delta y}\right) + F_\theta + Q \quad (3)$$

where $\left(\frac{\delta\theta}{\delta x}\right)$ and $\left(\frac{\delta\theta}{\delta y}\right)$ are the cross- and along- front temperature gradients, respectively, and Q is a diabatic term.

We can rewrite (2) as:

$$\frac{dD}{dt} = f(q - q_g) - \frac{1}{2}D^2 - \frac{1}{2}\delta^2 + \frac{1}{2}q^2 + F_D \quad (4)$$

where δ is the total deformation. F_q and F_D are the curl and divergence of the vertical shear of the Reynolds stresses:

$$F_q = (\tau_y)_{zx} - (\tau_x)_{zy} \quad (5)$$

$$F_D = (\tau_x)_{zx} + (\tau_y)_{zy} \quad (6)$$

where the shear of the stress can be expressed using K closure and Monin-Obukov theory (e.g., Garrat 1992).

In a homogeneous flow, F_q is a stress curl that generally acts to directly decrease the vorticity, whereas F_D generally acts to decrease the convergence. However, in a frontal region, the contributions from stratification and temperature advection induce additional indirect effects (Bannon and Salem, 1995). For example, SST variation could generate vorticity and divergence by itself through enhanced mixing on the cold air-side of the front and also through thermally induced circulations (the latter are probably unimportant compared with those associated with the synoptic activity). However, stronger downward mixing of momentum on the cold air-side of the front could induce significant convergence. At the same time, the stronger winds would increase the drag, which would also be enhanced by unstable conditions and young wave age over water.

These terms and effects can be determined by synergistic combination of observations from remote sensors, model analyses and ABL formulations as is illustrated in the case study presented in section 3. The observation of the stress field by Scatterometer and Synthetic Aperture Radar (SAR) (using a direct signal-to-stress algorithm) allows for a superior estimation and modelling of the stress terms (4)-(6).

2.2 Ageostrophy

The first term on the RHS of equation (4), $f(q-q_g)$, is the ageostrophic term. Along with the vortex stretching term (first term on the RHS of equation 1) it represents the effect of secondary circulations and indirect frictional effects in the BL (Ekman pumping/suction).

The role of the ageostrophic term is further characterized by defining a diagnostic parameter (Levy and Bretherton, 1987; Levy 1989):

$$C \equiv q_g / q \quad (7)$$

Subject to the approximation noted by Bannon and Salem (1995) its deviation from 1.0 determines whether or not the ageostrohpic component acts to enhance frontogenesis through vortex stretching. Levy and Bretherton (1987) and Levy (1989) have modeled this parameter with an ABL model. Levy (1989) has also shown the dependence of the ageostrophic parameter on both baroclinicity and stratification, and how it explains some of the observed differences between cold and warm fronts. Here we determine its spatial and temporal distribution using scatterometer observations for a specific case of a strengthening front, testing whether it has a predictive value.

3. OBSERVATIONS AND ANALYSIS

We illustrate our analysis with an example of a front propagating eastward from a decaying parent low in the Gulf of Alaska depicted in Figure 1 as a series of SeaWinds-on-ADEOS II and QuikSCAT swaths. Isobars identify the parent low. The front itself shows as the line of maximum vorticity calculated from the scatterometer winds. The front drifts eastward and away from the parent low. The consecutive positions of the front are shown in a single plot in Figure 2. Note that the front keeps its overall shape over time, shortening only toward the end of the time series.

3.1 Vorticity and divergence

A crude way of estimating the strength of the front is to average the vorticity and divergence along the front. Following Levy and Bretherton (1987) and others, we define the front as the line of maximum vorticity (coinciding with minimum divergence and related to the temperature front through, e.g., equation (3) below). The average vorticity and convergence along those lines are shown to increase over the three days of interest in Figure 3, indicating that the front has severed from the parent low but is not decaying.

The terms f(q-qg), -(f+q)D and the nonlinear terms in equation (4) are evaluated directly from observations for the May 17, 2003 at 08:34 UTC case (first panel in Figure 1) .

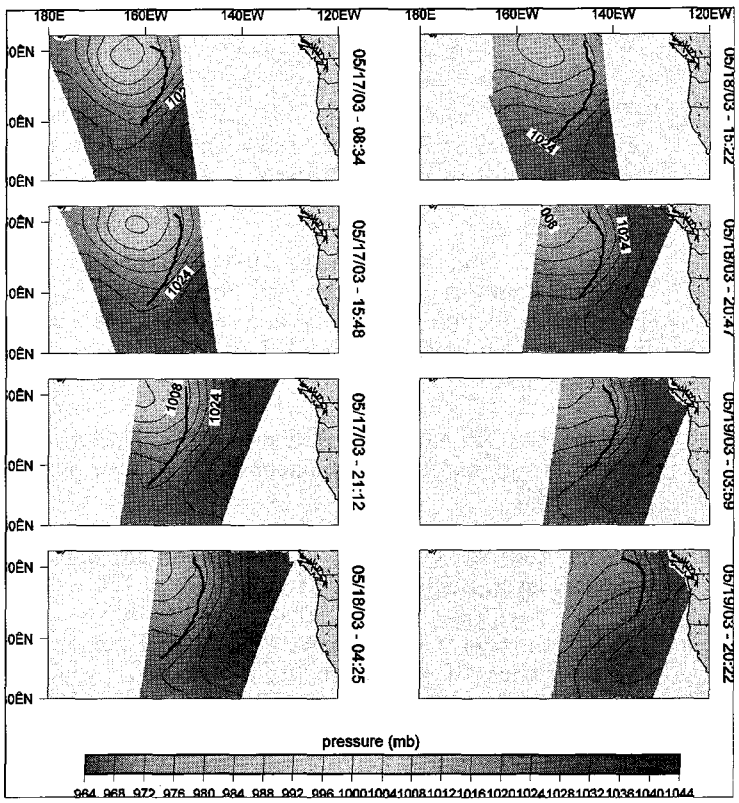

Figure 1. Cold front propagating eastward from parent low (May 17-19, 2003). The isobars are 4-hPa contours.

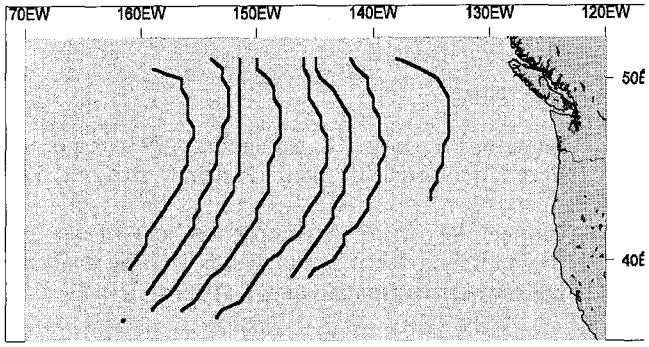

Figure 2. Cold front propagating eastward from parent low (May 17-19, 2003)

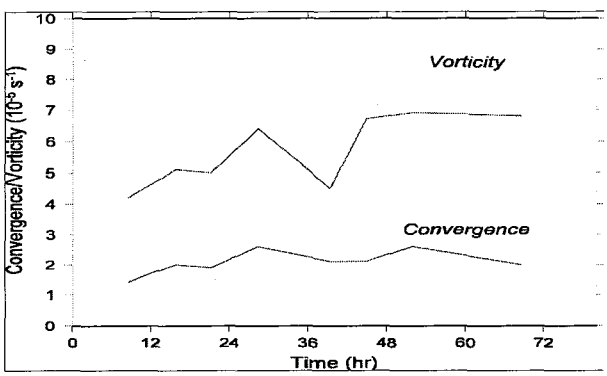

Figure 3. Average vorticity and convergence of the front

The evaluation of the term reveals that:

- The nonlinear terms are small and, if anything, increase the divergence in the low and part of the frontal region (closer to the low).
- f(q-qg) (ageostrophic term) and -(f+q)D (vortex stretching term) tend to increase the convergence and the vorticity respectively along the front and in the low. These terms represent the effect of secondary circulations and indirect frictional effects in the BL (Ekman pumping/suction).

3.2 Ageostrophy

An example of the analysis of the ageostrophic parameter (C) is shown in Figure 4a for the same front as above. The line of maximum vorticity as determined from NCEP surface winds at 06:00 UTC on May 17, 2003 is plotted in red. The blue colors show the regions where C is greater than 1. A SeaWinds swath at 08:34 allows us to determine the position of the cold front 2 hours later. The line of maximum vorticity as determined from the SeaWinds measurements is plotted in Figure 4b, overlaid on the same C surface as in Figure 4a for comparison. The cold front has moved toward the region where C is greater than 1 and reaches a maximum. It is thus proposed that the analysis of the different terms, even in a diagnostic sense, has predictive value, can shed light on the future evolution of a front, and be used as a forecasting tool.

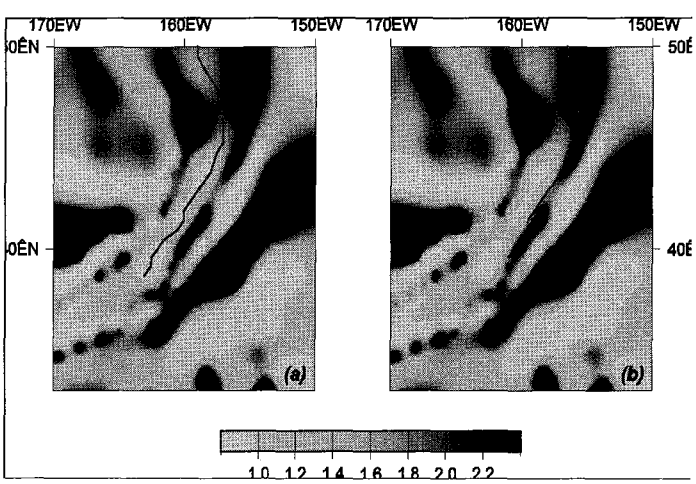

Figure 4. Evolution of the cold front toward the C>1 region. (a) Line of maximum vorticity from NCEP on May 17, 2003 at 6:00 UTC (b) Line of maximum vorticity from SeaWinds at 08:34 UTC (both panels) C calculated from NCEP at 6:00 UTC. Note that frontal features are revealed in vorticity analysis.

References

Bannon, P.R. and T.L. Salem Jr., 1995: Aspects of the Baroclinic Boundary Layer. J. Atmos. Sci., 52, 574-596.

Blumen, W., 1980: A comparison between the Hoskins-Bretherton model of frontogenesis and the analysis of an intense surface frontal zone, J. Atmos. Sci., 37, 64-77.

Garrat, J.R., 1992: The Atmospheric Boundary Layer. Cambridge University Press, Cambridge.

Hoskins, B.J., 1982: The mathematical theory of frontogenesis. Ann. Rev. Fluid Mech., 14, 131-151.

Hoskins, B.J. and F.P. Bretherton, 1972: Atmospheric frontogenesis models: Mathematical formulation and solution. J. Atmos. Sci., 29, 11-37.

Keyser, D. and Anthes, A., 1982: The influence of planetary boundary layer physics on frontal structure in the Hoskins-Bretherton horizontal shear model. , J. Atmos. Sci., 37, 1783-1802.

Keyser, D. and M.J. Pecknick, 1985: A two-dimensional primitive equation model of frontogenesis forced by confluence and horizontal shear. J. Atmos. Sci., 42, 1259-1282.

Levy, G., 1989: Surface dynamics of observed maritime fronts. J. Atmos. Sci., 46, 1219-1232.

Levy, G. and C.S. Bretherton, 1987: On the theory of the evolution of surface cold fronts. J. Atmos. Sci., 44, 3413-3418.

Reeder, M.J. and R.K. Smith, 1986: A comparison between frontogenesis in the two-dimensional Eady model of baroclinic instability and summertime cold fronts in the Australian region, Q. J. R. Meteorol. Soc., 112, 293-313.

Thompson, W.T. and R.T. Williams, 1997: Numerical simulations of maritime frontogenesis, J. Atmos. Sci., 54, 314-331.

Xu, Q. and W. Gu, 2002: Semigeostrophic frontal boundary layer, Bound.-Layer Meteor., 104, 99-110.

Yeh, H.-C., G.-J. Chen and W. Liu, 2002: Kinematic characteristics of a Mei-yu front detected by the QuikSCAT oceaninc winds. Mon. Wea. Rev., 130, 700-711.

Zierden, D.F., M.A. Bourassa and J.J. O'Brien, 2000: Cyclone surface pressure fields and frontogenesis from NASA scatterometer (NSCAT) winds. J. Geophys. Res., 105, 23,967-23,981.